Communications in Theoretical Physics

Commun. Theor. Phys. **77** (2025) 045201 (13pp) https://doi.org/10.1088/1572-9494/ad91b3

The effects of conical singularity and the Wu–Yang magnetic monopole on the thermodynamic properties of a harmonic oscillator interacting with a potential

Faizuddin Ahmed[1] **and Abdelmalek Bouzenada**[2]

[1] Department of Physics, University of Science & Technology Meghalaya, Ri-Bhoi, Meghalaya, 793101, India
[2] Laboratory of Theoretical and Applied Physics, Echahid Cheikh Larbi Tebessi University, Algeria

E-mail: faizuddinahmed15@gmail.com and abdelmalekbouzenada@gmail.com

Received 8 June 2024, revised 6 November 2024
Accepted for publication 7 November 2024
Published 20 December 2024

Abstract

In this work, we investigate the thermodynamic variables of a harmonic oscillator in a conical geometry metric. Moreover, we introduce an external field in the form of a Wu–Yang magnetic monopole (WYMM) and an inverse square potential into the system and analyze the results. Using an analytical approach, we obtain the energy level and study the thermodynamics at finite temperature. Our findings demonstrate that thermodynamic variables, except for the specific heat and entropy, are influenced by the topological parameters, the strength of the WYMM, and the inverse square potential.

Keywords: modified gravity theories, non-relativistic wave equations: harmonic oscillator, solutions of wave equations, bound-states, magnetic monopoles; special functions

1. Introduction

Quantum mechanics, a fundamental theory in physics, explains the physical characteristics of atoms and subatomic particles [1]. Unlike classical mechanics, which deals with macroscopic objects and aligns with everyday intuition, quantum mechanics operates on principles that often contradict classical intuition. A key concept in quantum mechanics is wave-particle duality [2], where particles like electrons exhibit both wave-like and particle-like properties. The behavior of these particles is governed by the Schrödinger equation [3], which provides a method for calculating the probability distribution of a particle's position and momentum [4].

Gravitational theory views gravity as the curvature of space-time rather than a force [5–7]. This perspective allows precise predictions of phenomena, such as the bending of light rays (gravitational lensing) [8–11] and gravitational waves. The current challenge in theoretical physics is the unification of quantum mechanics and general relativity theory [12–14]. While general relativity excels at describing the macroscopic world, it breaks down in extreme conditions where quantum effects are significant, such as inside black holes or at the beginning of the Universe. To address this, quantum gravity theories [15, 16], such as loop quantum gravity [17, 18] and string theory [19–21], have been developed in an attempt to create a unified framework that encompasses both of these fundamental aspects of modern physics.

Topological defects are irregularities or discontinuities that arise in ordered systems, frequently encountered in fields such as condensed matter physics and cosmology [22]. These defects emerge when the system's order parameters fail to maintain uniformity across space. Different types of topological defects [23] include: (i) domain walls [24], which are 2D surfaces separating regions of different phases; (ii) cosmic strings [25], which are 1D lines resembling cracks in space-time; (iii) monopoles [26], which are point-like defects carrying magnetic charge; (iv) textures [27], which are 3D configurations without a distinct core. Each type of defect has distinct physical implications and is characterized by specific topological properties [28]. In condensed matter systems,

such as liquid crystals and superconductors [29, 30], topological defects can significantly influence material properties and phase transitions [31]. In cosmology, these defects are believed to have formed during symmetry-breaking phase transitions in the early Universe, potentially affecting the large-scale structure of the cosmos [32]. However, the study of topological defects is constrained by the difficulty in detecting and observing them directly, especially in high-energy and large-scale contexts. Additionally, theoretical models must address the complexities of non-linear dynamics [33] and quantum field theory [34] to fully describe these defects.

In quantum systems, a harmonic oscillator serves as an analogue model of a classical harmonic oscillator [35]. Progressing further, the study of the harmonic oscillator within the context of curved space has been explored in only in a few works. These include investigations in the presence of conical singularities [36], in spaces with linear topological defects [37], the Aharonov–Bohm effect in 2D systems [38], the influence of singular potentials [39], within an elastic medium [40], and in the context of a global monopole [41, 42]. Understanding harmonic oscillators in curved space not only enriches our comprehension of classical mechanics but also provides valuable insights into the physical system in curved space. These insights have implications ranging from cosmology to quantum field theory [43].

The thermodynamic properties of quantum systems [44] exhibit different characteristics, which are distinct from those of classical systems [45]. Thermodynamic properties in quantum systems have been studied across various configurations. Notable examples include investigations in a Ga-As double ring-shaped quantum dot under external fields [46], in Rashba quantum dots with magnetic fields [47], and in asymmetric parabolic quantum dots [48, 49]. Other studies have explored these properties, such as within the framework of cosmic string space-time [50], relativistic quantum oscillators [51], and quantum oscillators with diatomic molecules [52]. Other research works in this direction are reported in [53–55].

Additional studies have focused on 1D Dirac oscillators [56], quantum fractional Dirac oscillators [57], and scalar bosons [58] in Rindler space-time. Research has also been conducted on deformed Dirac oscillators in one and two dimensions [59], the impact of minimal length effects on Dirac oscillators [60], Klein–Gordon (KG) oscillator in non-commutative space [61], and q-deformed relativistic Dirac oscillators with minimal length considerations [62]. Moreover, the properties of a 3D Dirac oscillator in non-commutative space [63] and with an Aharonov–Bohm field and magnetic monopole potential [64], anharmonic oscillators under cosmic string effects [65], and systems in disclination backgrounds with different potentials [66–73] have been thoroughly investigated.

In the current study, the main motivation is to investigate the thermodynamics of a harmonic oscillator in a conical geometry under the influence of a Wu–Yang magnetic monopole (WYMM), and an inverse square potential. We solve the wave equation using special functions and obtain the energy levels in a compact form. Subsequently, the thermodynamic behavior of the harmonic oscillator is studied at $\mathrm{T} \neq 0$ and we obtain an expression of the partition function Z. We then calculate the thermodynamic variables, such as the vibrational free energy (F), the mean free energy (U), the specific heat ($\mathcal{C}$), and the entropy ($\mathcal{S}$) of the system. Our results show that thermodynamic variables get modified by the global monopole parameter, the strength of the WYMM, and the potential for a particular ℓ-state. In contrast, the specific heat capacity and entropy only depend on the topological parameter but are independent of the WYMM and the chosen potential.

This paper is organized as follows: in section 2, we solve the harmonic oscillator problem in a conical geometry without and with a potential. There, we study the thermodynamics of the system without a potential in section 2.1 and with a potential in section 2.2. Finally, our conclusions are presented in section 3.

2. Effects of conical singularity and WYMM under a potential on the harmonic oscillator system

We investigate the harmonic oscillator in a conical singularity metric and discuss the thermodynamic properties. Therefore, we begin this section by starting a conical singularity metric in the chart where (t, r, θ, ϕ) is given by [74] ($\mathrm{c} = 1 = \hbar = \mathrm{G}$)

$$\begin{aligned} \mathrm{d}s^2 &= -\mathrm{d}t^2 + \frac{\mathrm{d}r^2}{\alpha^2} + r^2(\mathrm{d}\theta^2 + \sin^2\theta\, \mathrm{d}\phi^2) \\ &= -\mathrm{d}t^2 + \mathrm{g}_{ij}\, \mathrm{d}x^{\mathrm{i}}\, \mathrm{d}x^{\mathrm{j}}, \end{aligned} \tag{1}$$

where α is the global monopole parameter. This space-time has recently attracted considerable attention within the context of quantum systems (see, for example, [75–86]).

The wave equation describing a harmonic oscillator in a quantum system under a potential V(r) is given by [86]

$$\left[-\frac{1}{2M}\frac{1}{\sqrt{\mathrm{g}}}\mathcal{D}_i(\mathrm{g}^{ij}\sqrt{\mathrm{g}}\,\mathcal{D}_j) + \frac{1}{2}M\,\omega^2\,\rho^2 + V(\boldsymbol{r}) \right]\Psi(\boldsymbol{r}) = E\,\Psi(\boldsymbol{r}),\ \mathcal{D}_i \equiv (\partial_i - \mathrm{i}\,e\,A_i), \tag{2}$$

where E is the energy, $\vec{A}$ is the three-vector potential, $\mathrm{g} = \det\ (\mathrm{g}_{ij})$, and $\Psi(\boldsymbol{r})$ is given by

$$\Psi(\boldsymbol{r}) = \mathrm{R}(r)\,\mathrm{Y}_{\ell',m'}(\theta, \phi), \tag{3}$$

with $\mathrm{Y}_{\ell',m'}$ given in [86, 89–91] and called the conical harmonics, and ℓ', m' are the effective quantum numbers.

By expressing the wave equation (2) in the background metric, equation (1), using the electromagnetic potential given in [86–88] and the function in equation (3), we obtain the following differential equation:

$$\mathrm{R}''(\mathrm{r}) + \frac{2}{r}\mathrm{R}'(\mathrm{r}) + \frac{1}{\alpha^2} \times \left[2\,M(E - V(r)) - \mathrm{M}^2\,\omega^2\,r^2 - \frac{\lambda'}{r^2} \right]\mathrm{R}(r) = 0. \tag{4}$$

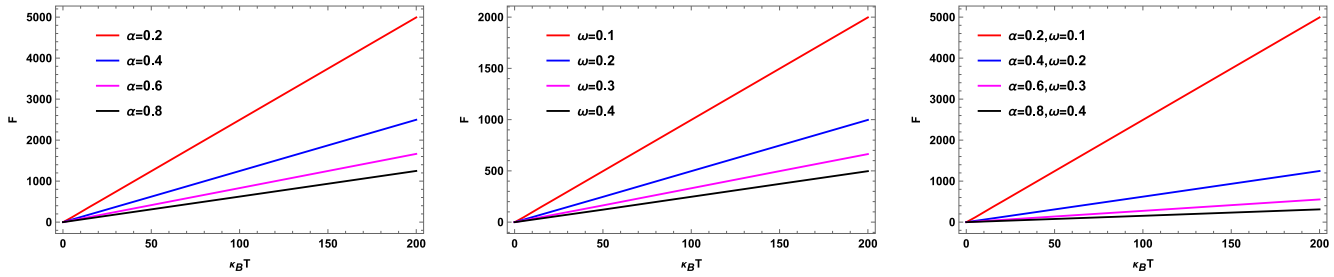

(a) $\omega = 0.1$ (b) $\alpha = 0.5$ (c)

Figure 1. (a)–(c) The partition function, equation (13), for the $\ell = 1$-state. Here, M = 1 and $\sigma = 0.1$.

Below, we focus on the thermal properties of the harmonic oscillator and discuss the effects of topological defects, the strength of the WYMM, and the potential depth, if there.

2.1. Thermodynamics of the harmonic oscillator without a potential

For zero potential, V(r) = 0, the radial equation (4) becomes

$$\mathrm{R}''(r) + \frac{2}{r}\,\mathrm{R}'(r) + \frac{1}{\alpha^2}\left[2\,M\,E - \Omega^2\,r^2 - \frac{\lambda'}{r^2}\right]\mathrm{R}(r) = 0. \tag{5}$$

Performing $\mathrm{R}(r) = \frac{\psi(r)}{\sqrt{r}}$, $s = \Omega\,r^2$ with $\Omega = M\,\omega$, and choosing the following function

$$\psi(s) = s^{\frac{\tau}{2}}\exp\left(-\frac{s}{2}\right){}_1\mathrm{F}_1(a,\,b;\,s) \tag{6}$$

in equation (5) results in the confluent hypergeometric differential equation form given by [92]

$$s\,\mathrm{F}''(s) + (b - s)\mathrm{F}'(s) - a\,\mathrm{F}(s) = 0, \tag{7}$$

where the function ${}_1\mathrm{F}_1$(a, b; s) is called the hypergeometric function and we defined

$$a = \tau + \frac{1}{2} - \frac{\Lambda}{4\,\Omega}, \quad b = \tau + 1,$$
$$\Lambda = \frac{2\,M\,E}{\alpha^2}, \quad \tau = \sqrt{\frac{\ell(\ell+1) - \sigma^2}{\alpha^2} + \frac{1}{4}}. \tag{8}$$

Its well-known in mathematical physics that the hypergeometric function ${}_1\mathrm{F}_1$(a, b; s) becomes a finite degree polynomial provided the relation is a = − n, where $n = 0, 1, 2, \ldots$. Simplification of $a = -n$ gives us the energy level as follows [86]:

$$\mathrm{E}_{n\,\ell\,\sigma} = 2\left(\mathrm{n} + \sqrt{\frac{\ell(\ell+1) - \sigma^2}{\alpha^2} + \frac{1}{4}} + \frac{1}{2}\right)\alpha\,\omega. \tag{9}$$

The wave function can then be written as

$$\mathrm{R}_{n\,\ell\,\sigma}(s) = \Omega^{1/4}\,s^{\frac{1}{2}\left(-\frac{1}{2} + \sqrt{\frac{\ell(\ell+1)-\sigma^2}{\alpha^2} + \frac{1}{4}}\right)}$$
$$\times\,\mathrm{e}^{-s/2}\,{}_1\mathrm{F}_1\left(-n,\,1 + \sqrt{\frac{\ell(\ell+1) - \sigma^2}{\alpha^2} + \frac{1}{4}};\,s\right). \tag{10}$$

Equations (9) and (10), respectively, are the energy levels and the radial function of the harmonic oscillator in topological defect geometry and a WYMM without any potential effects.

To study thermal properties, we now calculate the partition function Z(β) at $T \neq 0$ by utilizing the energy expression equation (9). Subsequently, we will calculate other physical quantities, such as the vibrational energy, the mean free energy, the specific heat capacity, and the entropy, and analyze the outcomes. Here, β is related with the absolute temperature T as $\beta = \frac{1}{k_{\mathrm{B}}\,T}$, where k_{B} is the Boltzmann constant.

The energy expression, equation (9), keeping ℓ and σ constant, is given by:

$$E_n = p\,n + q, \;\; p = 2\,\alpha\,\omega, \;\; q = (1 + 2\,\tau)\alpha\,\omega. \tag{11}$$

Partition Function

The partition function of a system at finite temperature is obtained using the definition [93–96]

$$\mathrm{Z} = \sum_{n=0}^{n=\infty} \mathrm{e}^{-\beta\,E_n}. \tag{12}$$

Using the energy expression, equation (11), we obtain the partition function given by:

$$\mathrm{Z}(\alpha,\,\omega,\,\sigma,\,T) = \frac{\exp\left[-\left(\frac{2\,\alpha\,\omega}{k_{\mathrm{B}}\,T}\right)\sqrt{\frac{\ell(\ell+1)-\sigma^2}{\alpha^2} + \frac{1}{4}}\right]}{2\sinh\left(\frac{\alpha\,\omega}{k_{\mathrm{B}}\,T}\right)}. \tag{13}$$

We see that Z depends on the topological parameter α, and σ, for a particular ℓ-state. Additionally, it varies with the absolute temperature T and the oscillator frequency ω. The behavior of Z as a function of $k_{\mathrm{B}}\,T$ is illustrated in figure 1 for different values of α and ω. We see that as the values of these parameters increase, the linear increase shifts downward in the range $0 \leqslant k_{\mathrm{B}}\,T \leqslant 200$.

Vibrational Free Energy

This is defined in terms of the partition function Z as follows:

$$\mathrm{F} = -\frac{1}{\beta}\,\ln\mathrm{Z}. \tag{14}$$

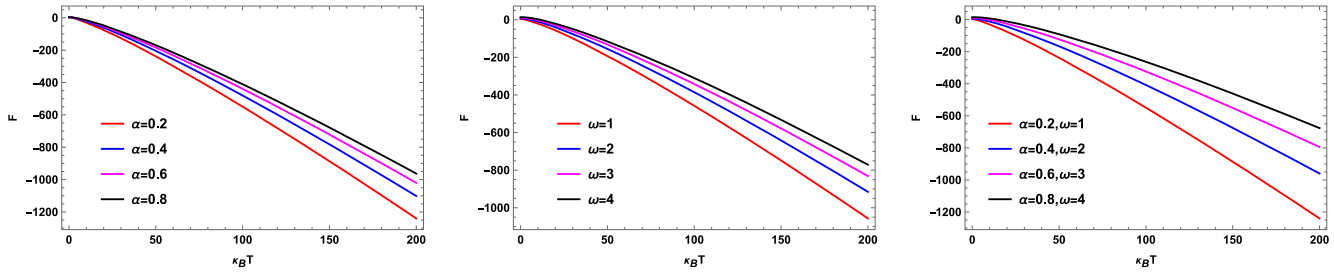

(a) $\omega = 1$ (b) $\alpha = 0.5$ (c)

Figure 2. (a)–(c) The vibrational free energy, equation (15), for the $\ell = 1$-state. Here, $\mathrm{M} = 1$ and $\sigma = 0.1$.

Using the partition function expression, equation (12), we obtain the vibrational free energy given by

$$\mathrm{F}(\alpha,\,\omega,\,\sigma,\,T) = \alpha\,\omega\left[2\sqrt{\frac{\ell(\ell+1)-\sigma^2}{\alpha^2}+\frac{1}{4}} + \frac{k_{\mathrm{B}}\,T}{\alpha\,\omega}\ln\left(2\sinh\left(\frac{\alpha\,\omega}{k_{\mathrm{B}}\,T}\right)\right)\right]. \tag{15}$$

We see that this energy depends on the topological parameter α, and the strength of the WYMM σ, for a particular ℓ-state. Additionally, it varies with the absolute temperature T and the oscillator frequency ω. In figure 2, the behavior of the vibrational free energy, equation (15), is plotted as a function of $k_{\mathrm{B}}\,T$ for different values of α and ω. It is evident that as the values of these parameters increase, the almost linear decrease shifts downward in the range $0 \leqslant k_{\mathrm{B}}\,T \leqslant 200$.

Writing $x = \frac{k_{\mathrm{B}}\,T}{\alpha\,\omega}$, the asymptotic form of the second term within the bracket in equation (15) for $x \to 0$ becomes $x\,\ln[2\sinh(1/x)] \approx 1$. Therefore, in the limit $\mathrm{T} \to 0$, the asymptotic form of the vibrational free energy will be

$$\mathrm{F}(\alpha,\,\omega,\,\sigma) \approx \left[2\sqrt{\frac{\ell(\ell+1)-\sigma^2}{\alpha^2}+\frac{1}{4}}+1\right]\alpha\,\omega. \tag{16}$$

Helmholtz Free Energy

This is defined by

$$\mathrm{U} = -\frac{\partial}{\partial\beta}(\ln \mathrm{Z}). \tag{17}$$

Using expression (13), we obtain this energy given by

$$\mathrm{U}(\alpha,\,\omega,\,\sigma,\,T) = \alpha\,\omega\left[2\sqrt{\frac{\ell(\ell+1)-\sigma^2}{\alpha^2}+\frac{1}{4}} + \coth\left(\frac{\alpha\,\omega}{k_{\mathrm{B}}\,T}\right)\right]. \tag{18}$$

We see that this Helmholtz free energy depends on the topological parameter α, and the strength of the WYMM σ, for a particular ℓ-state. Moreover, It changes with the absolute temperature T and the oscillator frequency ω. The behavior of this energy, equation (18), as a function of $\frac{1}{k_{\mathrm{B}}\,T}$ is plotted in figure 3 for different values of α and ω. It is evident that as the values of these parameters increase, the linear increase shifts downward in $k_{\mathrm{B}}\,T > 0$ (figure 3(a)–(b)). While in figure 3(c), it shows decreases in the nature of the curve in the range $k_{\mathrm{B}}\,T > 0$.

In the limit $T \to 0$, the asymptotic form of $\coth\left(\frac{\alpha\,\omega}{k_{\mathrm{B}}\,T}\right)$ is given by

$$\coth\left(\frac{\alpha\,\omega}{k_{\mathrm{B}}\,T}\right) \approx 1 + 2\,\mathrm{e}^{-\frac{2\,\alpha\,\omega}{k_{\mathrm{B}}\,T}}. \tag{19}$$

Therefore, the asymptotic form of the Helmholtz energy in the limit $T \to 0$ will be

$$\mathrm{U}(\alpha,\,\omega,\,\sigma,\,T) \approx \left[2\sqrt{\frac{\ell(\ell+1)-\sigma^2}{\alpha^2}+\frac{1}{4}}+1+2\,\mathrm{e}^{-\frac{2\,\alpha\,\omega}{k_{\mathrm{B}}\,T}}\right]\alpha\,\omega. \tag{20}$$

Specific Heat Capacity

This is defined by

$$\frac{\mathcal{C}}{k_{\mathrm{B}}} = \beta^2\,\frac{\partial^2}{\partial\beta^2}(\ln \mathrm{Z}). \tag{21}$$

Using expression (13), we obtain the specific heat capacity given by

$$\frac{\mathcal{C}(\alpha,\,\omega,\,T)}{k_{\mathrm{B}}} = \frac{\alpha^2\,\omega^2}{k_{\mathrm{B}}^2\,T^2}\,\frac{1}{\sinh^2\left(\frac{\alpha\,\omega}{k_{\mathrm{B}}\,T}\right)}. \tag{22}$$

One can see that the heat capacity depends only on the topological parameter α for a particular ℓ-state and changes with the absolute temperature T and the oscillator frequency ω. In figure 4, the behavior of the specific heat capacity, equation (22), is plotted as a function of $\frac{1}{k_{\mathrm{B}}\,T}$ for different values of α and ω. It is evident that as the values of these parameters increase, the nature of the decreasing curves shifts downward in the range $k_{\mathrm{B}}\,T > 0$.

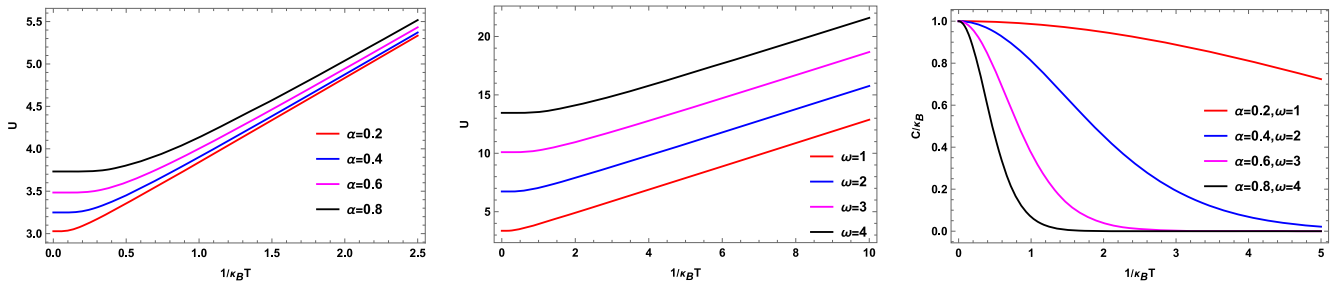

(a) $\omega = 1$ (b) $\alpha = 0.5$ (c)

Figure 3. (a)–(c) The Helmholtz free energy, equation (18), for the $\ell = 1$-state. Here, $\mathrm{M} = 1$ and $\sigma = 0.1$.

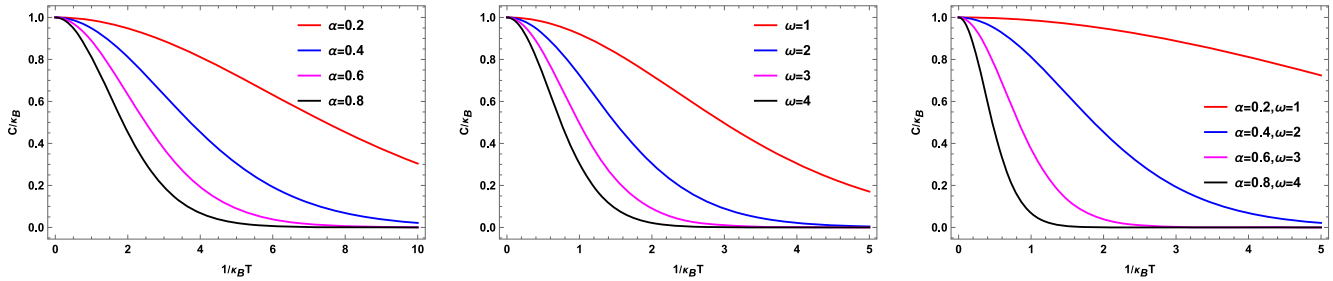

(a) $\omega = 1$ (b) $\alpha = 0.5$ (c)

Figure 4. (a)–(c) The specific heat capacity of equation (22).

Writing $x = \frac{k_{\mathrm{B}}\, T}{\alpha\, \omega}$, equation (22) can be written as

$$\frac{\mathcal{C}(\alpha,\, \omega,\, T)}{k_{\mathrm{B}}} = \frac{1}{x^2\, \sinh^2\left(\frac{1}{x}\right)}. \tag{23}$$

In the limit $x \to 0$, the asymptotic expansion of the above equation is given by

$$\frac{\mathcal{C}(\alpha,\, \omega,\, T)}{k_{\mathrm{B}}} \approx \left(\frac{2\, \alpha\, \omega}{k_{\mathrm{B}}\, T}\right)^2 \mathrm{e}^{-\frac{2\, \alpha\, \omega}{k_{\mathrm{B}}\, T}}. \tag{24}$$

This shows that the specific heat capacity decays very rapidly due to the exponential factor.

We have generated figure 6 showing this asymptotic form of the specific heat capacity as a function of $\kappa_{\mathrm{B}}\, T$ for different values of the topological parameter $0 < \alpha \leqslant 1$, keeping the frequency $\omega = 0.1 > 0$ fixed. It is clear from this figure that this vanishes as T approaches zero.

Entropy

This is defined by

$$\frac{\mathcal{S}}{k_{\mathrm{B}}} = \mathrm{lnZ} - \beta\, \frac{\partial}{\partial \beta}(\mathrm{lnZ}). \tag{25}$$

Using expression (13), we obtain the entropy of the system given by

$$\frac{\mathcal{S}(\alpha,\, \omega,\, T)}{k_{\mathrm{B}}} = \frac{\alpha\, \omega}{k_{\mathrm{B}}\, T} \coth\left(\frac{\alpha\, \omega}{k_{\mathrm{B}}\, T}\right) - \ln\left[2\, \sinh\left(\frac{\alpha\, \omega}{k_{\mathrm{B}}\, T}\right)\right]. \tag{26}$$

We see that the entropy of the system depends only on the topological parameter α for a particular ℓ-state and changes with the absolute temperature T and the oscillator frequency ω . In figure 5, the entropy behavior, equation (26), is plotted as a function of $k_{\mathrm{B}}\, T$ and observed to be parabolic in nature. It is evident that as the values of these parameters increase, the parabolic nature shifts downward in the range $0 \leqslant k_{\mathrm{B}}\, T \leqslant 200$.

Writing $x = \frac{k_{\mathrm{B}}\, T}{\alpha\, \omega}$, equation (26) can be written as

$$\frac{\mathcal{S}(\alpha,\, \omega,\, T)}{k_{\mathrm{B}}} = \frac{\coth\left(\frac{1}{\mathrm{x}}\right)}{\mathrm{x}} - \ln\left[2\, \sinh\left(\frac{1}{\mathrm{x}}\right)\right]. \tag{27}$$

In the limit $x \to 0$, the asymptotic expansion of entropy is given by

$$\frac{\mathcal{S}(\alpha,\, \omega,\, T)}{k_{\mathrm{B}}} \approx \frac{2\, \alpha\, \omega}{k_{\mathrm{B}}\, T}\, \mathrm{e}^{-\frac{2\, \alpha\, \omega}{k_{\mathrm{B}}\, T}}. \tag{28}$$

This shows that entropy of the quantum system decays exponentially as T approaches zero.

We have generated figure 7 showing this asymptotic form of entropy as a function of $\kappa_{\mathrm{B}}\, T$ for different values of the topological parameter $0 < \alpha \leqslant 1$, keeping the frequency $\omega = 0.1 > 0$ fixed. It is clear from this figure that entropy vanishes as T approaches zero.

In summary, we have examined the thermodynamics of a harmonic oscillator without a potential in a conical geometry and in a WYMM. Figures (1)–(7) illustrate how thermodynamic variables, such as the partition function, the vibrational free energy, the Helmholtz free energy, the specific heat capacity, and entropy, are influenced by various parameters. These figures demonstrate the dependence of thermodynamic

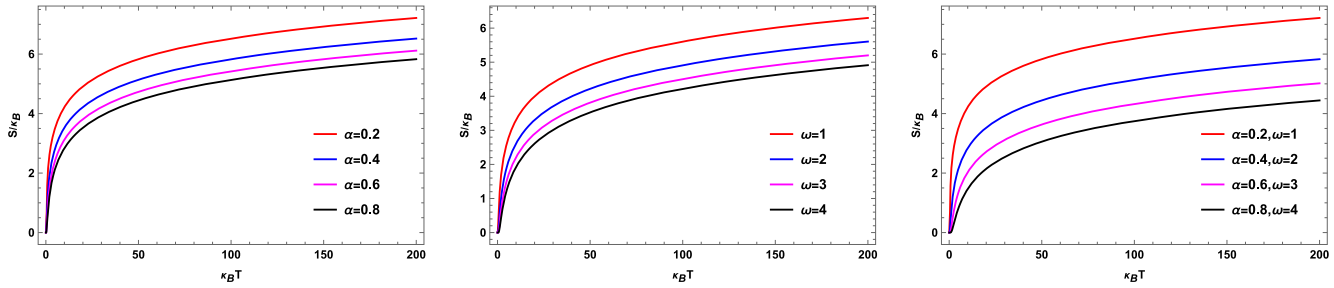

(a) $\omega = 1$ (b) $\alpha = 0.5$ (c)

Figure 5. (a)–(c) The entropy of equation (26).

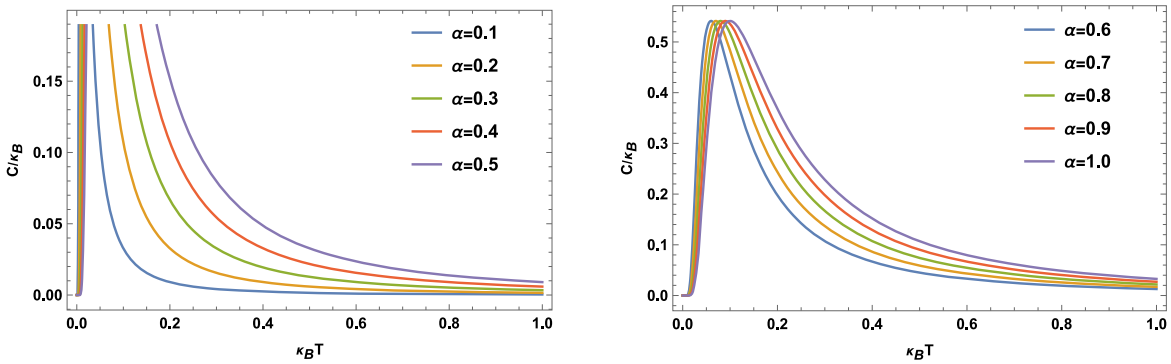

Figure 6. The behavior of the asymptotic specific heat capacity as a function of T. Here, $\omega = 0.1$.

variables on the topological parameter α, and the strength of the WYMM σ. Notably, we have observed that the specific heat capacity and entropy of the system are independent of the strength of the WYMM.

2.2. Thermodynamics of the harmonic oscillator with a potential

Here, we consider an inverse square potential $\mathrm{V}(r) = \frac{\eta}{r^2}$, where $\eta > 0$ is a constant. Using this potential, we find the radial equation as follows:

$$\mathrm{R}''(r) + \frac{2}{r}\,\mathrm{R}'(r) + \left[\frac{2\,M\,E}{\alpha^2} - \Omega^2\,r^2 - \frac{\lambda' + 2\,M\,\eta}{\alpha^2\,r^2}\right] \times \mathrm{R}(r) = 0. \tag{29}$$

Performing $\mathrm{R}(r) = \frac{\psi(r)}{\sqrt{r}}$, $s = \Omega\,r^2$ with $\Omega = \mathrm{M}\,\omega$, and inserting the following function

$$\psi(s) = s^{\iota/2}\exp(-s/2)\,{}_1\mathrm{F}_1(c, d; s) \tag{30}$$

into equation (29) results in the confluent hypergeometric differential equation form [92] given by

$$s\,\mathrm{F}''(s) + (\mathrm{d} - s)\mathrm{F}'(s) - \mathrm{c}\,\mathrm{F}(s) = 0, \tag{31}$$

with ${}_1\mathrm{F}_1(c, d, s)$ called the confluent hypergeometric function, and we define

$$c = \iota + \frac{1}{2} - \frac{\Lambda}{4\,\Omega}, \quad d = 1 + \iota,$$
$$\iota = \sqrt{\frac{\ell(\ell+1) - \sigma^2 + 2\,\mathrm{M}\,\eta}{\alpha^2} + \frac{1}{4}}. \tag{32}$$

Following the previous procedure and after some calculation, we find the energy levels given by

$$E_{n\,\ell\sigma} = 2\left(n + \sqrt{\frac{\ell(\ell+1) - \sigma^2 + 2\,\mathrm{M}\,\eta}{\alpha^2} + \frac{1}{4}} + \frac{1}{2}\right)\alpha\,\omega. \tag{33}$$

The radial function is given by

$$\mathrm{R}_{n\,\ell\sigma}(s) = \Omega^{1/4}\,s^{\frac{1}{2}\left(-\frac{1}{2} + \sqrt{\frac{\ell(\ell+1)-\sigma^2+2\,\mathrm{M}\,\eta}{\alpha^2} + \frac{1}{4}}\right)} \times e^{-s/2}\,{}_1\mathrm{F}_1\left(-n,\, 1 + \sqrt{\frac{\ell(\ell+1) - \sigma^2 + 2\,\mathrm{M}\,\eta}{\alpha^2} + \frac{1}{4}};\, s\right). \tag{34}$$

Equation (33) is the energy level and equation (34) is the radial function of the harmonic oscillator in the conical metric and in a WYMM under the influence of an inverse square potential. We see that the energy level is influenced by various factors, such as the strength of the WYMM (σ), the topological parameter (α), and the potential parameter (η).

Here, we will also study thermal properties at $T \neq 0$ and analyze the results. The energy expression, equation (33),

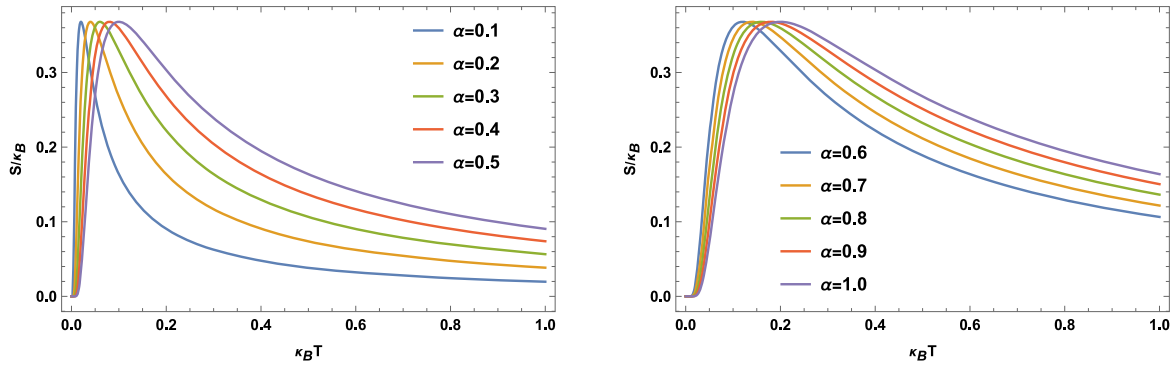

Figure 7. The behavior of the asymptotic entropy form as a function of T. Here, $\omega = 0.1$

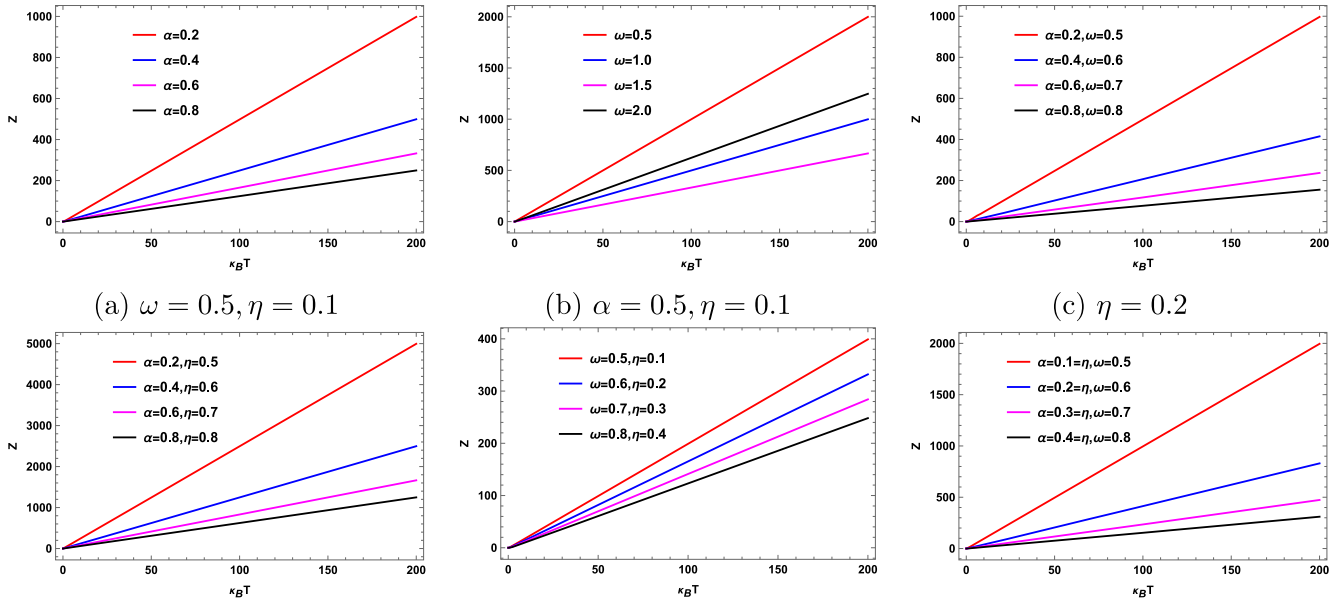

(a) $\omega = 0.5, \eta = 0.1$ (b) $\alpha = 0.5, \eta = 0.1$ (c) $\eta = 0.2$

(d) $\omega = 0.1$ (e) $\alpha = 0.5$ (f)

Figure 8. (a)–(f) The partition function, equation (36), for the $\ell = 0$-state. Here, $\mathrm{M} = 1$ and $\sigma = 0.1$.

keeping ℓ and σ constant, can be written as

$$\mathrm{E}_n = p\, n + \tilde{q},\ \ p = 2\,\alpha\,\omega,\ \ \tilde{q} = (1 + 2\,\iota)\alpha\,\omega. \tag{35}$$

Using the above energy expression, equation (35), we obtain the partition function given by

$$\mathrm{Z}(\alpha,\,\omega,\,\sigma,\,\eta,\,T) = \frac{\exp\left[-\frac{2\,\alpha\,\omega}{k_{\mathrm{B}}\,T}\sqrt{\frac{\ell(\ell+1)-\sigma^2+2\,\mathrm{M}\,\eta}{\alpha^2}+\frac{1}{4}}\right]}{2\,\sinh\left(\frac{\alpha\,\omega}{k_{\mathrm{B}}\,T}\right)}. \tag{36}$$

The partition function Z depends on several parameters: the topological parameter α, the strength of the WYMM σ, and the potential strength η for a particular ℓ-state. Additionally, It varies with the absolute temperature T and the oscillator frequency ω. The behavior of this function, equation (36), for $\ell = 0$- and $\ell = 1$-states is illustrated in figures (8) and (9). As shown, the partition function exhibits a linear relationship with $k_{\mathrm{B}}\,T > 0$ for specific values of $(\alpha,\,\omega)$. This linear trend shifts downward with increasing values of α, $\omega\,\eta$, while keeping σ fixed.

Vibrational Free Energy

The vibrational free energy using equation (36) is given by

$$\mathrm{F}(\alpha,\,\omega,\,\sigma,\,\eta,\,T) = 2\,\alpha\,\omega\sqrt{\frac{\ell(\ell+1)-\sigma^2+2\,\mathrm{M}\,\eta}{\alpha^2}+\frac{1}{4}} + k_{\mathrm{B}}\,T\,\ln\left[2\,\sinh\left(\frac{\alpha\,\omega}{k_{\mathrm{B}}\,T}\right)\right]. \tag{37}$$

This energy depends on several factors, such as the topological parameter α, the strength of the WYMM σ, and the potential strength η for a particular ℓ-state. Moreover, it changes with the absolute temperature T and the oscillator frequency ω. The behavior of this energy, equation (37) for $\ell = 0$ and $\ell = 1$-states is depicted in figures (10) and (11). It is clear from these figures that this energy decreases with increasing $k_{\mathrm{B}}\,T$ for particular values of α, ω, and η. These decreasing trends shift upward with increasing values of the aforementioned parameters in the range $0 < k_{\mathrm{B}}\,T \leqslant 5$.

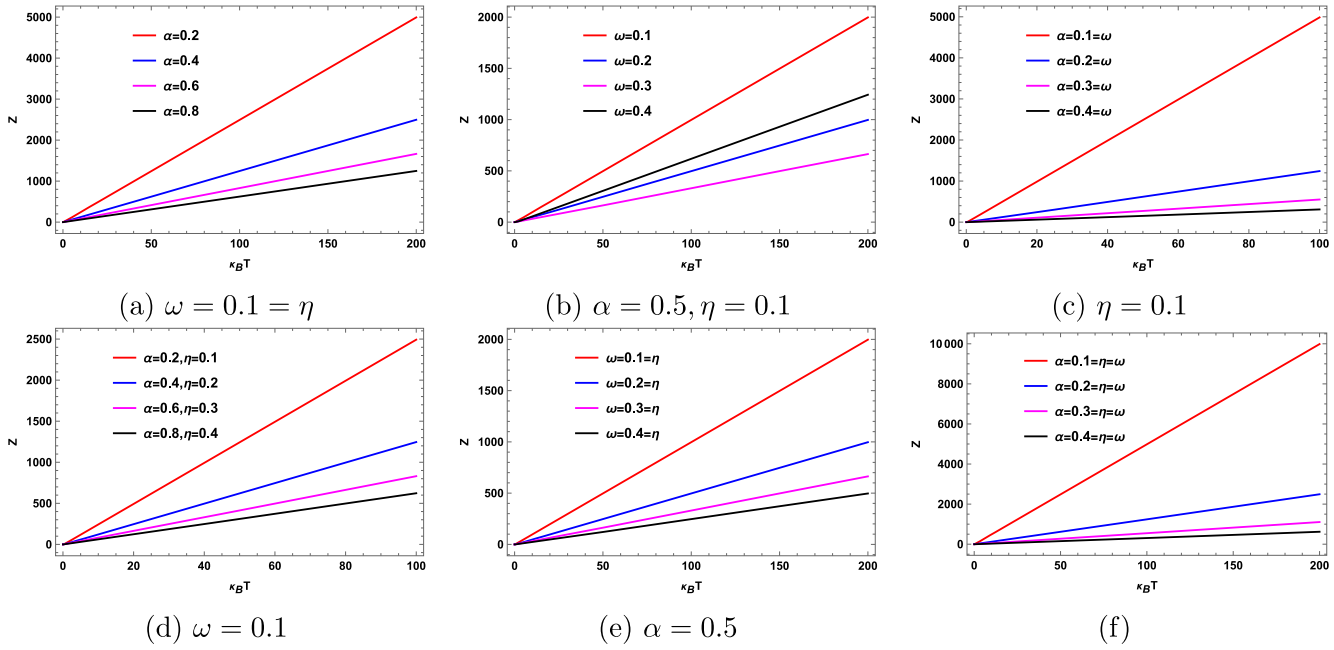

(a) $\omega = 0.1 = \eta$ (b) $\alpha = 0.5, \eta = 0.1$ (c) $\eta = 0.1$

(d) $\omega = 0.1$ (e) $\alpha = 0.5$ (f)

Figure 9. (a)–(f) The partition function, equation (36), for the $\ell = 1$-state. Here, $\mathrm{M} = 1$ and $\sigma = 0.1$.

In the limit $T \to 0$, the asymptotic form of the vibrational free energy is given by

$$\mathrm{F}(\alpha,\, \omega,\, \sigma,\, \eta) \approx \left[2\,\sqrt{\frac{\ell(\ell+1) - \sigma^2 + 2\,\mathrm{M}\,\eta}{\alpha^2}} + \frac{1}{4}\right] + 1\,\alpha\,\omega. \tag{38}$$

Helmholtz Free Energy

The mean energy using equation (36) is given by

$$\mathrm{U}(\alpha,\, \omega,\, \sigma,\, \eta,\, T) = \alpha\,\omega\left[2\,\sqrt{\frac{\ell(\ell+1) - \sigma^2 + 2\,\mathrm{M}\,\eta}{\alpha^2}} + \frac{1}{4} + \coth\left(\frac{\alpha\,\omega}{k_{\mathrm{B}}\,T}\right)\right]. \tag{39}$$

The Helmholtz energy depends on the topological parameter α, the strength of the WYMM σ, and the potential strength η for a particular ℓ-state. Additionally, it varies with the absolute temperature T and the oscillator frequency ω. The behavior of the Helmholtz energy, equation (39), for $\ell = 0$- and $\ell = 1$-states is illustrated in figures (12) and (13). As shown, this energy is almost linear with increasing $\frac{1}{k_{\mathrm{B}}\,T}$ for particular values of α, ω, and η. This linear trend shifts upward with increasing values of these parameters $(\alpha,\, \omega,\, \eta)$ when $\frac{1}{k_{\mathrm{B}}\,T} > 0$.

The asymptotic form of Helmholtz energy in the limit $T \to 0$ becomes

$$\mathrm{U}(\alpha,\, \omega,\, \sigma,\, \eta,\, T) \approx \alpha\,\omega\left[2\,\sqrt{\frac{\ell(\ell+1) - \sigma^2 + 2\,\mathrm{M}\,\eta}{\alpha^2}} + \frac{1}{4} + 1 + 2\,\mathrm{e}^{-\frac{2\,\alpha\,\omega}{k_{\mathrm{B}}\,T}}\right]. \tag{40}$$

Specific Heat Capacity

Using expression (36), we find the specific heat capacity given by

$$\frac{\mathcal{C}(\alpha,\, \omega,\, T)}{k_{\mathrm{B}}} = \left(\frac{\alpha\,\omega}{k_{\mathrm{B}}\,T}\right)^2 \frac{1}{\sinh^2\left(\frac{\alpha\,\omega}{k_{\mathrm{B}}\,T}\right)}, \tag{41}$$

which is similar to the previous result, equation (22).

The specific heat capacity depends only on the topological parameter α for a particular ℓ-state. Additionally, it changes with the absolute temperature T and the oscillator frequency ω. Interestingly, it is independent of the potential and the WYMM interaction. Therefore, its behavior closely resembles that depicted in figure 4.

Entropy

Using expression (13), we obtain the entropy of the system given by

$$\frac{\mathcal{S}(\alpha,\, \omega,\, T)}{k_{\mathrm{B}}} = \frac{\alpha\,\omega}{k_{\mathrm{B}}\,T}\coth\left(\frac{\alpha\,\omega}{k_{\mathrm{B}}\,T}\right) - \ln\left[2\,\sinh\left(\frac{\alpha\,\omega}{k_{\mathrm{B}}\,T}\right)\right], \tag{42}$$

which is similar to the previous result, equation (26).

This entropy depends only on the topological parameter α for a particular ℓ-state. Moreover, it changes with the absolute temperature T and the oscillator frequency ω. Interestingly, we see that it is independent of the potential and the WYMM interaction. Therefore, its behavior closely resembles that depicted in figure 5.

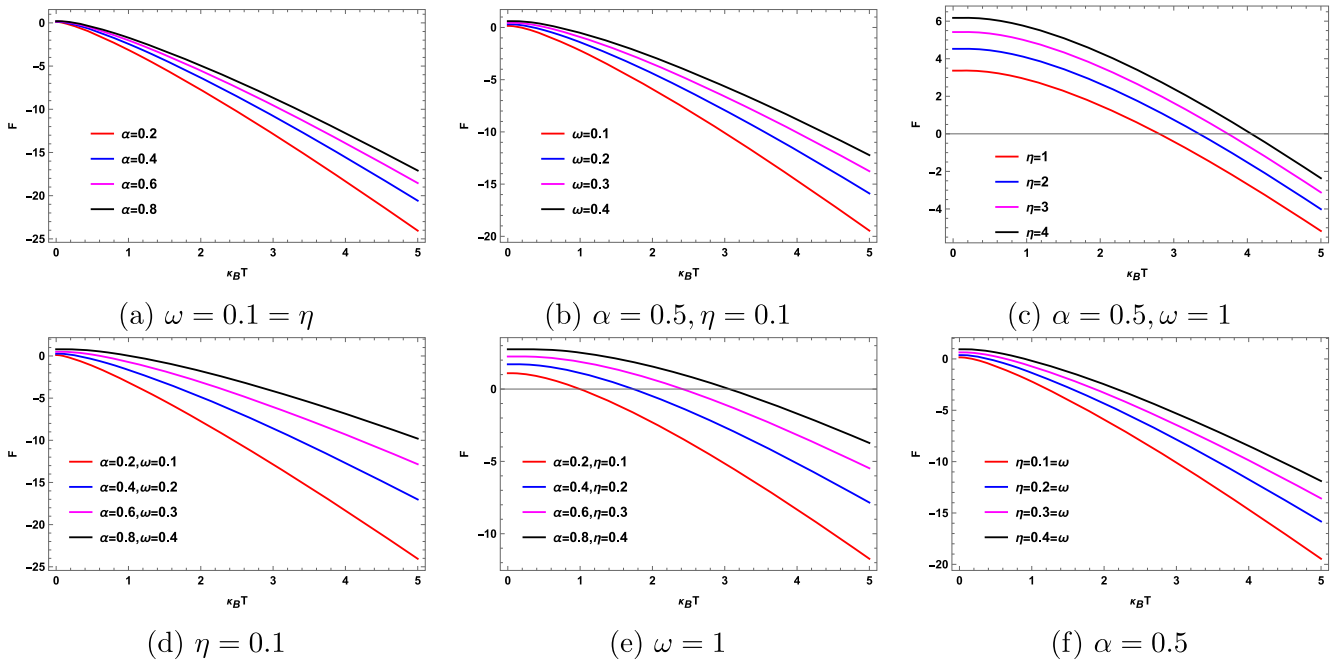

(a) $\omega = 0.1 = \eta$ (b) $\alpha = 0.5, \eta = 0.1$ (c) $\alpha = 0.5, \omega = 1$

(d) $\eta = 0.1$ (e) $\omega = 1$ (f) $\alpha = 0.5$

Figure 10. (a)–(f) The vibrational free energy, equation (37), for the $\ell = 0$-state. Here, M = 1 and $\sigma = 0.1$.

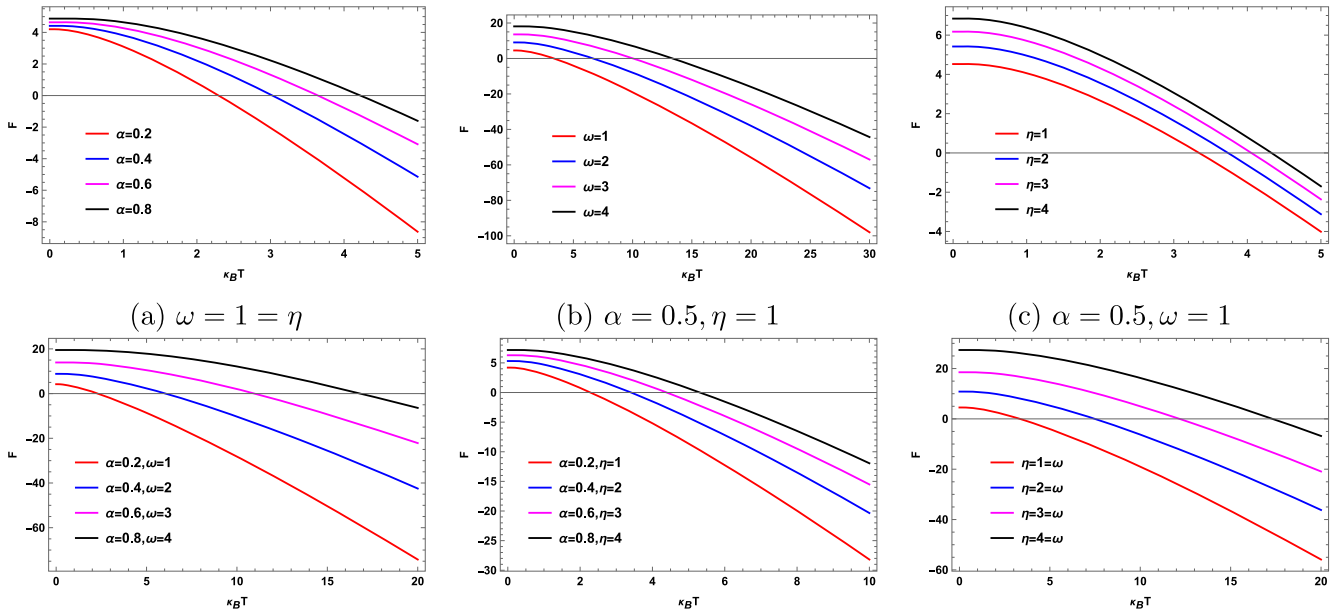

(a) $\omega = 1 = \eta$ (b) $\alpha = 0.5, \eta = 1$ (c) $\alpha = 0.5, \omega = 1$

(d) $\eta = 1$ (e) $\omega = 1$ (f) $\alpha = 0.5$

Figure 11. (a)–(f) The vibrational free energy, equation (37), for the $\ell = 1$-state. Here, M = 1 and $\sigma = 0.1$.

In summary, we have examined the thermal properties of a harmonic oscillator under potential effects in a conical metric and in a WYMM. Figures (8)–(13) illustrate how thermodynamic variables, such as the partition function, vibrational free energy, Helmholtz free energy, specific heat capacity, and entropy are influenced by. These figures demonstrate the dependence of thermodynamic variables on the topological parameter α, the strength of the WYMM σ, and the potential strength η. Notably, we have observed that the specific heat capacity and entropy are independent of the potential and the strength of the WYMM.

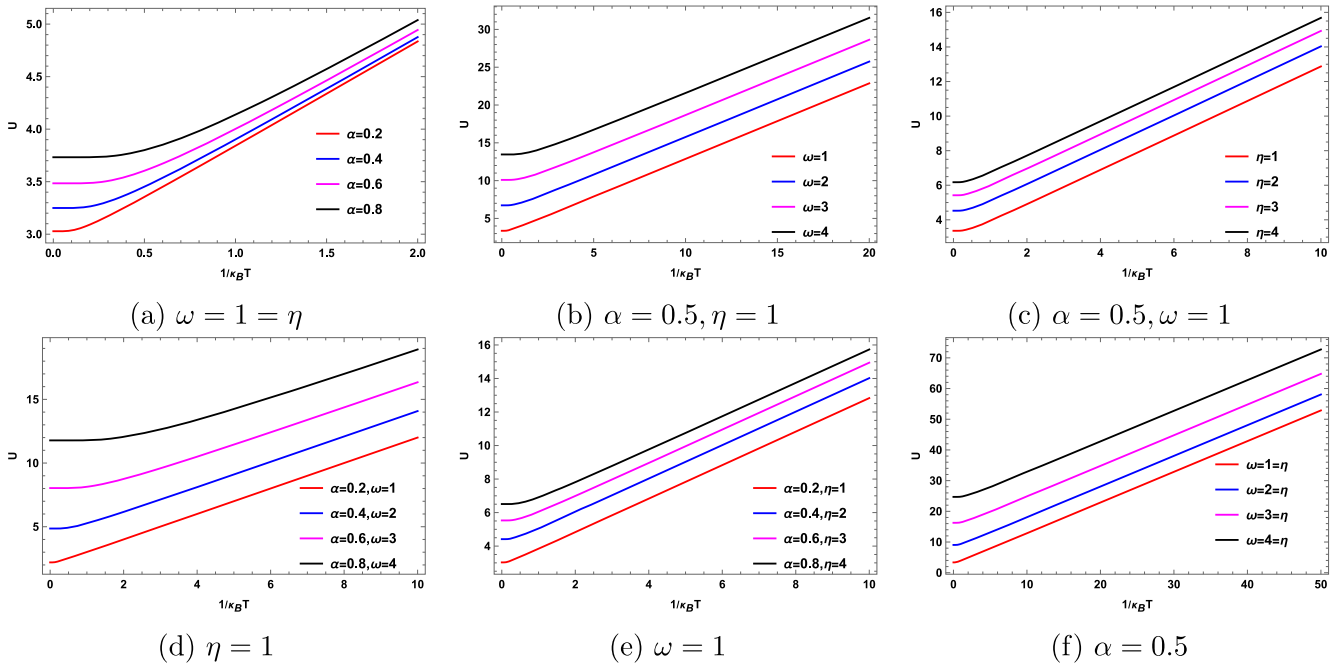

(a) $\omega = 1 = \eta$ (b) $\alpha = 0.5, \eta = 1$ (c) $\alpha = 0.5, \omega = 1$

(d) $\eta = 1$ (e) $\omega = 1$ (f) $\alpha = 0.5$

Figure 12. (a)–(f) The Helmholtz free energy, equation (39), for the $\ell = 0$-state. Here, $\alpha = 0.5$, $\omega = 1$.

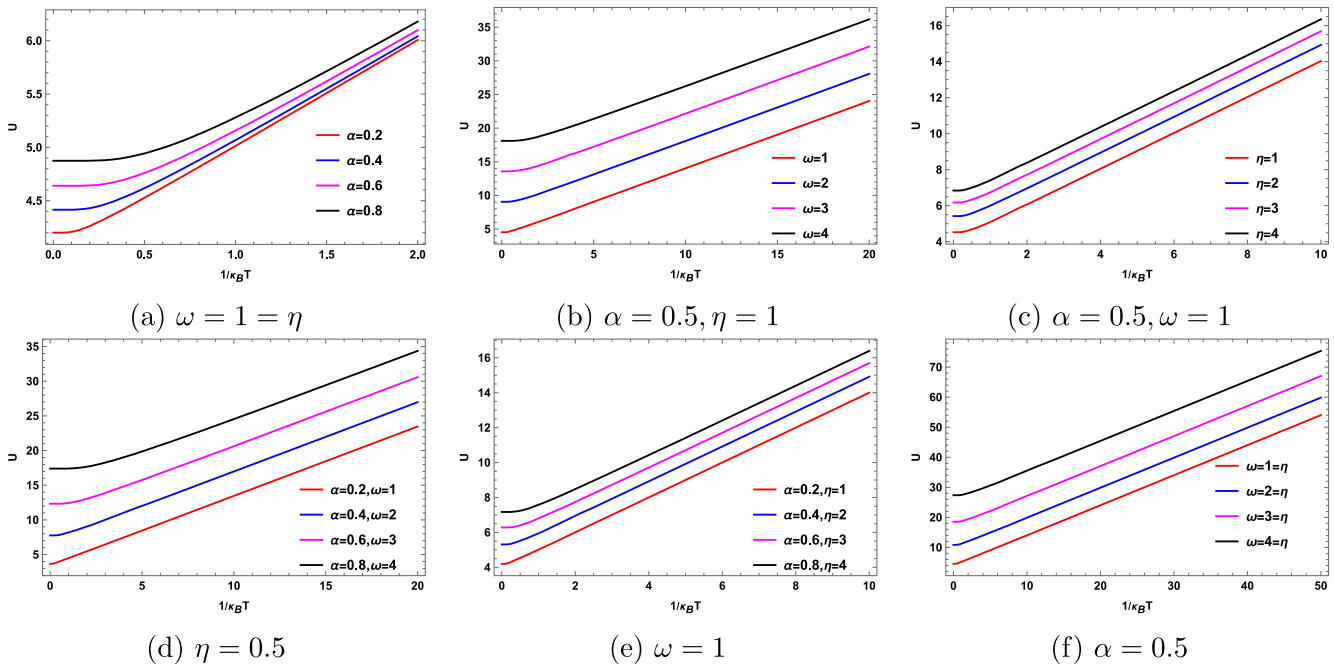

(a) $\omega = 1 = \eta$ (b) $\alpha = 0.5, \eta = 1$ (c) $\alpha = 0.5, \omega = 1$

(d) $\eta = 0.5$ (e) $\omega = 1$ (f) $\alpha = 0.5$

Figure 13. (a)–(f) The Helmholtz free energy, equation (39), for the $\ell = 1$-state. Here, $\alpha = 0.5$, $\omega = 1$.

3. Conclusions

In this current work, we examined the thermodynamic properties of a harmonic oscillator in a conical metric and a WYMM under a potential. We solved the wave equation and obtained a compact form of the energy levels and the radial wave function using special functions, both without and with a potential.

In section 2.1, we studied the thermodynamics of the system without a potential and obtained thermodynamic variables, including the partition function, the vibrational free energy, the Helmholtz free energy, the specific heat capacity, and entropy. It has been demonstrated that these variables, except for the specific heat capacity and entropy, depend on the topological parameter α and the strength of the WYMM σ. We depicted several figures illustrating the behavior of these variables as a function of $\frac{1}{\beta} = k_{\mathrm{B}}\, T$ for different values of the aforementioned parameters, including the oscillator frequency.

In section 2.2, we introduced an inverse square potential and studied the thermodynamics of the system. Similar to the previous section, we analyzed the partition function, the vibrational free energy, the Helmholtz free energy, the specific heat capacity, and entropy. We have demonstrated that these physical quantities vary with the potential in addition to those parameters mentioned earlier in the previous paragraph. Again, it was observed that the specific heat capacity and entropy are independent of the strength of the WYMM and the potential. We have provided graphs illustrating the behavior of these thermodynamic variables as a function of $\frac{1}{\beta} = k_{\rm B}\, T$ for different values of various parameters.

The investigation into the thermodynamics of a harmonic oscillator in conical geometry, featuring a WYMM and an inverse square potential, provided intriguing insights into the interplay between quantum mechanics and a classical thermodynamic system. Through rigorous analysis, we have elucidated the impact of the global monopole parameter characterized by α. Moreover, the presence of the WYMM introduces non-trivial magnetic interactions, altering the dynamics of the harmonic oscillator and, thereby, changing the thermodynamic behavior. Additionally, the inclusion of an inverse square potential modified the solution of the wave equation, leading to changes in the thermodynamic properties.

We have depicted several figures (figures (1)–(13)) illustrating the partition function, vibrational energy, Helmholtz energy, specific heat capacity, and entropy as functions of $k_{\rm B}\, T$ and, in some cases, $\frac{1}{k_{\rm B}\, T}$ for specific values of (α, ω, η) while keeping the WYMM strength σ and ℓ constant. Additionally, we have varied the values of these parameters to demonstrate how they influence the behavior of these thermodynamic functions.

These findings not only deepen our theoretical understanding of quantum systems in the presence of topological defects but also pave the way for potential applications in diverse fields, ranging from condensed matter physics to quantum information processing. Notably, we have observed that the specific heat capacity and entropy are independent of both the potential and the strength of the WYMM.

In our upcoming work, we will investigate the quantum equipartition theorem as it applies to the current system, following the approach outlined in [97]. We will also analyze the results obtained from this study and discuss the effects of conical singularity and the WYMM.

Acknowledgments

We sincerely acknowledge the anonymous referees for their valuable remarks and suggestions. FA acknowledges the Inter University Centre for Astronomy and Astrophysics (IUCAA), Pune, India for granting a visiting associateship.

ORCID iDs

Faizuddin Ahmed https://orcid.org/0000-0003-2196-9622
Abdelmalek Bouzenada https://orcid.org/0000-0002-3363-980X

References

[1] Greiner W 2011 *Quantum Mechanics: An Introduction* (Berlin: Springer)
[2] Yang C D 2005 Wave-particle duality in complex space *Ann. Phys.* **319** 444
[3] Schrödinger E 1926 Quantisierung als Eigenwertproblem *Ann. Phys.* **385** 437
[4] Hofmann H F 2017 Quantum interference of position and momentum: a particle propagation paradox *Phys. Rev.* A **96** 020101(R)
[5] Einstein A 1916 Die Grundlage der allgemeinen Relativitätstheorie *Ann. Phys.* **354** 769
[6] Einstein A, Infeld L and Hoffmann B 1938 The gravitational equations and the problem of motion *Ann. Math.* **39** 65
[7] Robertson H P 1949 Postulate versus observation in the special theory of relativity *Rev. Mod. Phys.* **21** 378
[8] Turyshev S G 2024 Gravitational lensing for interstellar power transmission *Phys. Rev.* D **109** 064029
[9] Chen Y, Wang P, Wu H and Yang H 2024 Gravitational lensing by Born–Infeld naked singularities *Phys. Rev.* D **109** 084014
[10] Sarkar N, Sarkar S, Bouzenada A, Dutta A, Sarkar M and Rahaman F 2024 Traversable wormholes with weak gravitational lensing effect in $f(R, T)$ gravity *Phys. Dark Univ.* **44** 101439
[11] Grespan M and Biesiada M 2023 Strong gravitational lensing of gravitational waves: a review *Universe* **9** 200
[12] Tamm M 2023 Different aspects of spin in quantum mechanics and general relativity *Symmetry* **15** 2016
[13] Socolovsky M 2023 Hidden quantum effect in general relativity *J. High Energy Phys.* **9** 913
[14] Gemsheim S and Rost J M 2023 Emergence of time from quantum interaction with the environment *Phys. Rev. Lett.* **131** 140202
[15] Eichhorn A, Santos R R L D and Miqueleto J L 2024 From quantum gravity to gravitational waves through cosmic strings *Phys. Rev.* D **109** 026013
[16] Harlow D and Ooguri H 2021 Symmetries in quantum field theory and quantum gravity *Commun. Math. Phys.* **383** 1669
[17] Ashtekar A and Bianchi E 2021 A short review of loop quantum gravity *Rep. Prog. Phys.* **84** 042001
[18] Bojowald M and Duque E I 2024 Inequivalence of mimetic gravity with models of loop quantum gravity *Phys. Rev.* D **109** 084044
[19] Schwarz J H 1982 Superstring theory *Phys. Rep.* **89** 223
[20] Witten E 1995 String theory dynamics in various dimensions *Nucl. Phys.* B **443** 85
[21] Zurek W H 1996 Cosmological experiments in condensed matter systems *Phys. Rep.* **276** 177
[22] Barkeshli M, Jian C M and Qi X L 2013 Classification of topological defects in Abelian topological states *Phys. Rev.* B **88** 241103
[23] Catalan G, Seidel J, Ramesh R and Scott J F 2012 Domain wall nanoelectronics *Rev. Mod. Phys.* **84** 119
[24] Bennett D P and Bouchet F R 1989 Cosmic-string evolution *Phys. Rev. Lett.* **63** 2776
[25] Carrigan R A Jr. and Trower W P 1983 Magnetic monopoles *Nature* **305** 673
[26] Brandenberger R H 1994 Topological defects and structure formation *Int. J. Mod. Phys.* A **9** 2117
[27] Cortijo A and Vozmediano M A 2007 Effects of topological defects and local curvature on the electronic properties of planar graphene *Nucl. Phys.* B **763** 293
[28] Laflorencie N 2016 Quantum entanglement in condensed matter systems *Phys. Rep.* **646** 1–59

[29] Halperin B I and Lubensky T C 1974 On the analogy between smectic a liquid crystals and superconductors *Solid State Commun.* **14** 997
[30] Vilenkin A and Shellard E P S 1994 *Cosmic Strings and Other Topological Defects* (Cambridge: Cambridge University Press)
[31] Armas J and Jain A 2024 Approximate higher-form symmetries, topological defects, and dynamical phase transitions *Phys. Rev.* D **109** 045019
[32] Dudek H J 2023 Action origin of the cosmos *J. High Energy Phys. Gravit. Cosmol.* **9** 850
[33] Skogvoll V, Rønning J, Salvalaglio M and Angheluta L 2023 A unified field theory of topological defects and non-linear local excitations *Npj Comput. Mater.* **9** 122
[34] Itzykson C and Zuber J B 1980 *Quantum Field Theory* (New York: McGraw-Hill)
[35] Bloch S C 2013 *Introduction to Classical and Quantum Harmonic Oscillators* (New York: Wiley)
[36] Furtado C and Moraes F 2000 Harmonic oscillator interacting with conical singularities *J. Phys. A: Math. Gen.* **33** 5513
[37] Azevedo S 2001 Harmonic oscillator in a space with a linear topological defect *Phys. Lett.* A **288** 33
[38] Azevedo S 2002 Topological Aharonov–Bohm effect in a two-dimensional harmonic oscillator *Phys. Lett.* A **293** 283
[39] Filgueiras C, Silva E O, Oliveira W and Moraes F 2010 The effect of singular potentials on the harmonic oscillator *Ann. Phys.* **325** 2529
[40] Maia A V D M and Bakke K 2018 Harmonic oscillator in an elastic medium with a spiral dislocation *Physica B: Cond. Matter* **531** 213
[41] Vitria R L L and Belich H 2019 Harmonic oscillator in an environment with a pointlike defect *Phys. Scr.* **94** 125301
[42] Ahmed F 2023 Harmonic oscillator problem in the background of a topologically charged Ellis–Bronnikov-type wormhole *Europhys. Lett.* **141** 54001
[43] Vergel D G and Villaseñor E J S 2009 The time-dependent quantum harmonic oscillator revisited: applications to quantum field theory *Ann. Phys.* **324** 1360
[44] Shankar R 2012 *Principles of Quantum Mechanics* (Berlin: Springer)
[45] Bender C M, Brody D C and Hook D W 2008 Quantum effects in classical systems having complex energy *J. Phys. A: Math. Theor.* **41** 352003
[46] Sukirti G, Kumar M, Jha P K and Mohan M 2016 Thermodynamic behaviour of Rashba quantum dot in the presence of magnetic field *Chin. Phys.* B **25** 056502
[47] Ibragimov G B 2003 Free-carrier magnetoabsorption in quantum well wires *Fizika* **34** 35
[48] Khordad R and RastegarSedehi H R 2018 Thermodynamic properties of a double ring-shaped quantum dot at low and high temperatures *J. Low. Temp. Phys.* **190** 200
[49] Khordad R and RastegarSedehi H R 2019 Magnetic susceptibility of graphene in non-commutative phase-space: extensive and non-extensive entropy *Eur. Phys. J. Plus* **134** 133
[50] Hassanabadi H and Hosseinpour M 2016 Thermodynamic properties of neutral particle in the presence of topological defects in magnetic cosmic string background *Eur. Phys. J.* C **76** 553
[51] Boumali A, Allouani R, Bouzenada A and Serdouk F 2023 Effect of the applied electric field on the thermal properties of the relativistic harmonic oscillator in one dimension *Ukr. J. Phys.* **68** 235
[52] Al-Raeei M, El-Daher M S, Bouzenada A and Boumali A 2023 A novel formula of equilibrium bond distance of the quantum oscillator with temperature dependence in diatomic molecules *Pramana* **97** 144
[53] Bouzenada A and Boumali A 2023 Statistical properties of the two dimensional Feshbach–Villars oscillator (FVO) in the rotating cosmic string space–time *Ann. Phys.* **452** 169302
[54] Bouzenada A, Boumali A and Serdouk F 2023 Thermal properties of the 2D Klein–Gordon oscillator in a cosmic string space–time *Theor. Math. Phys.* **216** 1055
[55] Boumali A, Bouzenada A, Zare S and Hassanabadi H 2023 Thermal properties of the q-deformed spin-one DKP oscillator *Physica A: Stat. Mech. Appl.* **628** 129134
[56] Rouabhia T I and Boumali A 2023 Statistical properties of the one-dimensional Dirac oscillator in Rindler space–time *Theor. Math. Phys.* **217** 1509
[57] Korichi N, Boumali A and Hassanabadi H 2022 Thermal properties of the one-dimensional space quantum fractional Dirac oscillator *Physica A: Stat. Mech. App.* **587** 126508
[58] Boumali A and Rouabhia T I 2021 The thermal properties of the one-dimensional boson particles in Rindler spacetime *Phys. Lett.* A **385** 126985
[59] Boumali A and Hassanabadi H 2017 The statistical properties of the q-deformed Dirac oscillator in one and two dimensions *Adv. High Energy Phys.* **2017** 9371391
[60] Boumali A, Chetouani L and Hassanabadi H 2016 Effect of a minimal length on the thermal properties of a Dirac oscillator *Acta Phys. Polon.* B **47** 2067
[61] Hassanabadi H, Hosseini S S, Boumali A and Zarrinkamar S 2014 The statistical properties of Klein–Gordon oscillator in noncommutative space *J. Math. Phys.* **55** 033502
[62] Hassanabadi H, Sargolzaeipor S and Yazarloo B H 2018 Statistical properties of the q-deformed relativistic Dirac oscillator in minimal length quantum mechanics *Can. J. Phys.* **96** 25
[63] Hassanabadi H, Hosseini S S, Ikot A N, Boumali A and Zarrinkamar S 2014 The chiral operators and the statistical properties of the $(2+1)$-dimensional Dirac oscillator in noncommutative space *Eur. Phys. J. Plus* **129** 232
[64] Hassanabadi H, Sargolzaeipor S and Yazarloo B H 2015 Thermodynamic properties of the three-dimensional Dirac oscillator with Aharonov–Bohm field and magnetic monopole potential *Few-Body Syst.* **56** 115
[65] Sobhani H, Hassanabadi H and Chung W S 2018 Effects of cosmic-string framework on the thermodynamical properties of anharmonic oscillator using the ordinary statistics and the q-deformed superstatistics approaches *Eur. Phys. J.* C **78** 106
[66] Ahmed F 2023 Thermodynamic properties and persistent currents of harmonic oscillator under AB-flux field in a point-like defect with inverse square potential *J. Low Temp. Phys.* **211** 11
[67] Ahmed F 2023 Effects of cosmic string on non-relativistic quantum particles with potential and thermodynamic properties *Int. J. Theor. Phys.* **62** 142
[68] Eshghi M, Sever R and Ikhdair S M 2019 Thermal and optical properties of two molecular potentials *Eur. Phys. J. Plus* **134** 155
[69] Eshghi M, Mehraban H and Ikhdair S M 2017 The relativistic bound states of a non-central potential *Pramana* **88** 73
[70] Eshghi M, Mehraban H and Azar I A 2017 Eigen spectra and wave functions of the massless Dirac fermions under the nonuniform magnetic fields in graphene *J. Phys.* E **94** 106
[71] Eshghi M, Mehraban H and Ahmadi Azar I 2017 Eigenspectra and thermodynamic quantities in graphene under the inside and outside magnetic fields *Eur. Phys. J. Plus* **132** 477
[72] Eshghi M and Mehraban H 2016 Non-relativistic continuous states in arbitrary dimension for a ring-shaped pseudo-Coulomb and energy-dependent potentials *Math. Meths. Appl. Sci.* **39** 1599
[73] Eshghi M and Hamzavi M 2018 Yukawa-like confinement potential of a scalar particle in a Gödel-type spacetime with any ℓ *Eur. Phys J.* C **78** 522

[74] Barriola M and Vilenkin A 1989 Gravitational field of a global monopole *Phys. Rev. Lett.* **63** 341
[75] de G, Marques A and Bezerra V B 2002 Non-relativistic quantum systems on topological defects spacetimes *Class. Quantum Grav.* **19** 985
[76] de G, Marques A, De Assis J G and Bezerra V B 2007 Some effects on quantum systems due to the gravitational field of a cosmic string *J. Math. Phys.* **48** 112501
[77] Ahmed F 2023 Point-like defect on Schrödinger particles under flux field with harmonic oscillator plus Mie-type potential: application to molecular potentials *Proc. R. Soc.* A **479** 20220624
[78] Nwabuzor P, Edet C, Ikot A N, Okorie U S, Ramantswana M, Horchani R, Aty A-H A and Rampho G 2021 analyzing the effects of topological defect (TD) on the energy spectra and thermal properties of *LiH*, *TiC* and I_2 diatomic molecules *Entropy* **23** 1060
[79] Ahmed F 2023 Topological effects on non-relativistic eigenvalue solutions under AB-flux field with pseudoharmonic-and Mie-type potentials *Commun. Theor. Phys.* **75** 055103
[80] Ahmed F 2023 Topological effects produced by point-like global monopole with Hulthen plus screened Kratzer potential on eigenvalue solutions and NU-method *Phys. Scr.* **98** 015403
[81] Ahmed F 2023 Eigenvalue spectra of non-relativistic particles confined by AB-flux field with Eckart plus class of Yukawa potential in point-like global monopole *Ind. J. Phys.* **97** 2307
[82] Ahmed F, Bouzenada A and Moreira A R P 2024 Effects of Pöschl–Teller potential on approximate $\ell \neq 0$-states solution in topological defect geometry and Shannon entropy *Phys. Scr.* **99** 075411
[83] Alves S S, F dos, Azevedo S, Filgueiras C and Silva E O 2024 Exact and approximate bound state solutions of the Schrödinger equation with a class of Kratzer-type potentials in the global monopole spacetime *Chin. J. Phys.* **88** 609
[84] Alves S S, Cunha M M, Hassanabadi H and Silva E O 2023 Approximate analytical solutions of the Schrödinger equation with Hulthén potential in the global monopole spacetime *Universe* **9** 132
[85] Bakke K 2023 Topological effects of a global monopole on the Hulthén potential *Eur. Phys. J. Plus* **138** 85
[86] Ahmed F and Bouzenada A 2024 Harmonic oscillator in topologically charged deformed gravity space–time and Wu–Yang magnetic monopole *Phys. Dark Universe* **46** 101690
[87] Wu T T and Yang C N 1975 Concept of nonintegrable phase factors and global formulation of gauge fields *Phys. Rev.* D **12** 3845
[88] Wu T T and Yang C N 1976 Dirac monopole without strings: monopole harmonics *Nucl Phys.* B **107** 365
[89] de Oliveira A L C and Bezerra de Mello E R 2003 Nonrelativistic scattering analysis of charged particle by a magnetic monopole in the global monopole background *Int. J. Mod. Phys.* A **18** 2051
[90] de Oliveira A L C and Bezerra de Mello E R 2005 Nonrelativistic quantum analysis of the charged particle–dyon system on a conical spacetime *Class. Quantum Grav.* **22** 1255
[91] de Oliveira A L C and Bezerra de Mello E R 2006 Exact solutions of the Klein–Gordon equation in the presence of a dyon, magnetic flux and scalar potential in the spacetime of gravitational defects *Class. Quantum Grav.* **23** 5249
[92] Abramowitz M and Stegun I A 1972 *Handbook of Mathematical Functions with Formulas, Graphs, and Mathematical Tables* (New York: Dover)
[93] Edet C O and Ikot A N 2021 Effects of topological defect on the energy spectra and thermo-magnetic properties of CO diatomic molecule *J. Low Temp. Phys.* **203** 84
[94] Edet C O *et al* 2022 Magneto-transport and thermal properties of the Yukawa potential in cosmic string space-time *Res. Phys.* **39** 105749
[95] Ikot A N, Okorie U S, Osobonye G, Amadi P O, Edet C O, Sithole M J, Rampho G J and Sever R 2020 Superstatistics of Schrödinger equation with pseudo-harmonic potential in external magnetic and Aharanov–Bohm fields *Heliyon* **6** e03738
[96] Jia C S, You X T, Liu J Y, Zhang L H, Peng X L, Wang Y T and Wei L S 2019 Prediction of enthalpy for the gases Cl_2, Br_2, and gaseous *Br Chem. Phys. Lett.* **717** 16
[97] Kaur J, Ghosh A and Bandyopadhyay M 2021 Quantum counterpart of energy equipartition theorem for a dissipative charged magneto-oscillator: effect of dissipation, memory, and magnetic field *Phys. Rev.* E **104** 064112